FRONTIERS IN NONLINEAR OPTICS

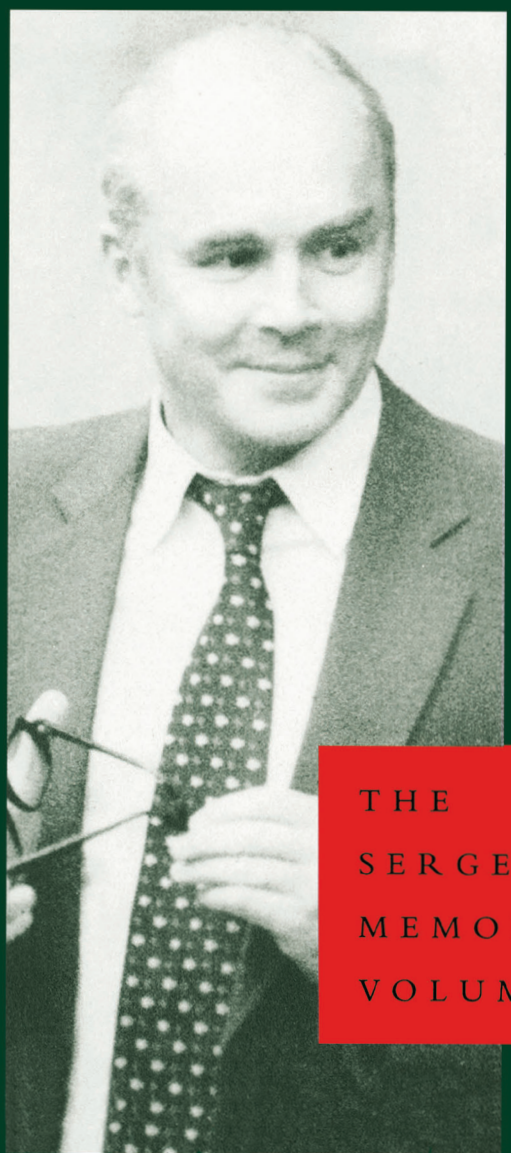

Edited by

H WALTHER

N KOROTEEV

M O SCULLY

Foreword by

NICO BLOEMBERGEN

THE SERGEI AKHMANOV MEMORIAL VOLUME

ONTIERS IN NONLINEAR OPTICS

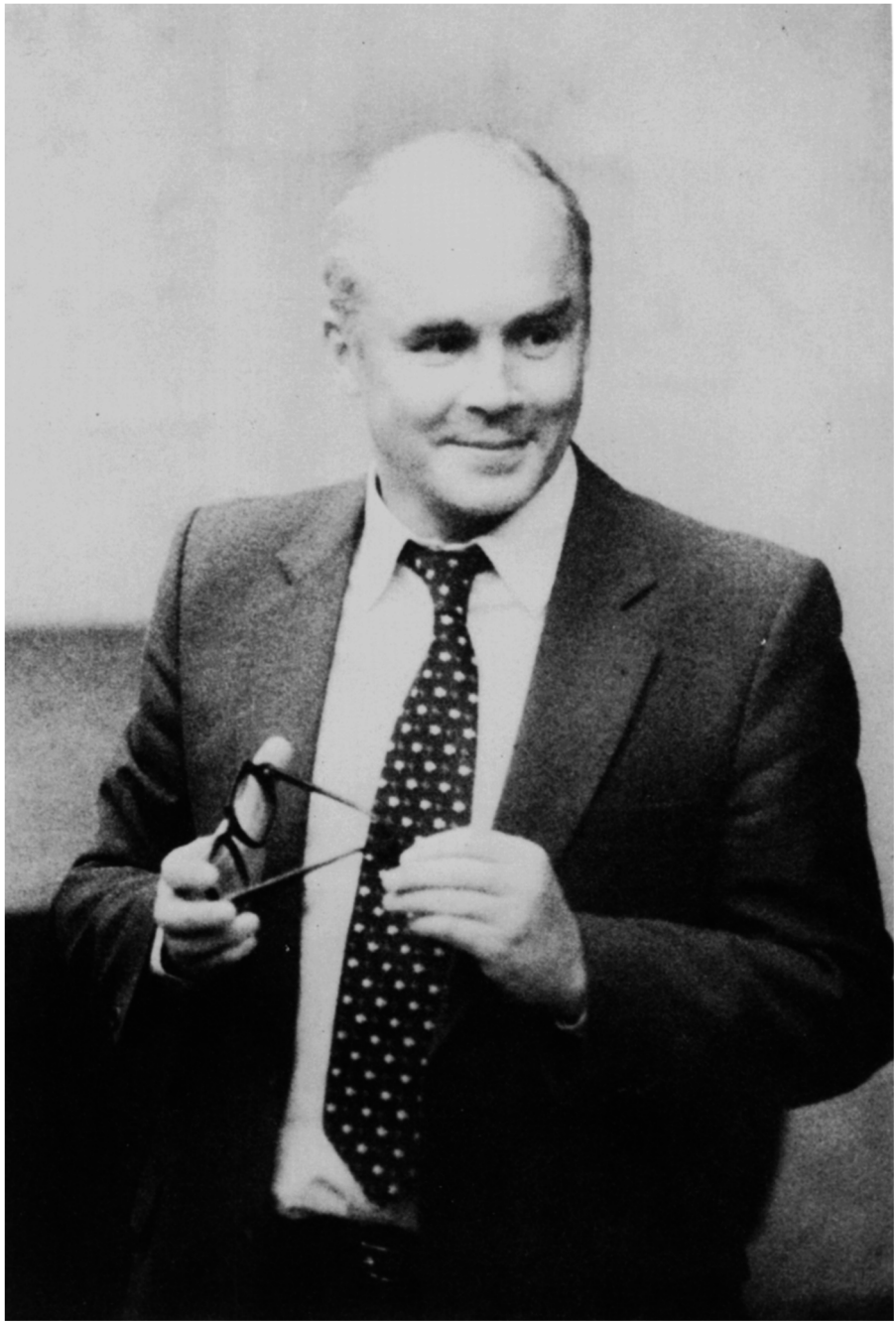

SERGEI ALEKSANDROVICH AKHMANOV 14 July 1929–1 July 1991

FRONTIERS IN NONLINEAR OPTICS

THE SERGEI AKHMANOV MEMORIAL VOLUME

Edited by
H WALTHER
Max-Planck-Institut für Quantenoptik, Garching

N KOROTEEV
Moscow State University, Moscow

M O SCULLY
University of New Mexico, Albuquerque

CRC Press
Taylor & Francis Group
Boca Raton London New York

CRC Press is an imprint of the
Taylor & Francis Group, an **informa** business

First published 1993 by lOP Publishing Ltd.

Published 2021 by CRC Press
Taylor & Francis Group
6000 Broken Sound Parkway NW, Suite 300
Boca Raton, FL 33487-2742

ISBN 13: 978-0-7503-0218-0 (hbk)
ISBN 13: 978-1-00-320963-8 (ebk)

DOI: 10.1201/9781003209638

Visit the Taylor & Francis Web site at
http://www.taylorandfrancis.com

and the CRC Press Web site at
http://www.crcpress.com

British Library Cataloguing in Publication Data
A catalogue record for this book is available from the British Library

Library of Congress Cataloging-in-Publication Data are available

ACKNOWLEDGMENT OF THE EDITORS

This volume is dedicated to the memory of our distinguished colleague Sergei Aleksandrovich Akhmanov, a pioneer in the field of nonlinear optics. The editors of this book would like to express their gratitude to all the contributors of this volume, due to their effort this book represents an in depth survey of the modern trends in nonlinear optics.

The Editors

FOREWORD

The untimely death of Sergei Aleksandrovich Akhmanov came as a shock not only to his family, friends and colleagues in Eastern Europe, but also to a large number of physicists around the globe. Many of them knew him personally, or enjoyed reading his scientific papers.

It is most appropriate that this volume with writings in the broad field of quantum electronics and non-linear optics be dedicated to his memory. Sergei, as we in the West called him, was indeed one of the pioneers in this field of scientific endeavour. I consider it a privilege to have been invited to write this foreword, and in this way to pay tribute to the memory of a dear friend and colleague.

On my first visit to the Soviet Union in 1967, I recall noticing a large mural, spontaneously drawn by a number of well-wishers in a hallway at Moscow State University, depicting Rem Khokhlov and Sergei Akhmanov as intrepid young horsemen conquering the fields of non-linear optics. They had just been awarded the Lenin Prize by the Soviet State in recognition of their pioneering contributions. They had entered this new field very early, recognizing it as a natural extension of their work in radiophysics during the late fifties which dealt with parametric interactions along microwave transmission lines. In 1972 and 1963 they gave a series of lectures on problems in non-linear optics, and their lecture notes were published in 1964 in a volume sponsored by the Soviet Academy of Sciences. At the same time I had prepared my lecture notes on Non-linear Optics for the 1964 Summer School in Les Houches. These were subsequently published as an independent monograph by W A Benjamin. Rem, Sergei and I exchanged autographed copies of our respective works. From that time Sergei and I continued to work independently on many closely related topics. We saw each other regularly at international meetings such as the series of International Quantum Electronic Conferences (IQEC), at several Gordon Research Conferences, at a Vavilov Conference in Novosibirsk in 1971, to name a few.

In particular I wish to recall a few memories about Sergei Akhmanov's participation at the E Fermi Course 64, at the July 1975 Summer School in Varenna, Italy. He gave fine lectures about three different topics: 'Coherent active spectroscopy of combinatorial scattering' (better known in the West as four-wave mixing spectroscopy or CARS), 'Higher-order optical non-linearities' (including fifth-harmonic generation in calcite), and 'Statistical effects in resonant non-linear optics' (optical and temporal multimode effects with random phases). One evening we planned a party and Sergei had brought vodka and caviar from Moscow. We needed, however, a hardboiled egg and fresh lemon. The former we readily obtained from the kitchen. Then Sergei and I took an evening stroll in the garden of the Villa Monastero along the shores of Lake Como. We walked along the decorative lemon trees. In the darkness we ignored the warning signs in Italian and each of us picked a forbidden fruit, a fresh lemon. This was the beginning of a marvelous evening party. Two aspects of Sergei's life are illustrated by this story. He was a leader in science, knowledgeable in a broad range of theoretical and experimental issues. At the same time, he was kind, cheerful, modest and generous. He always gave credit and referred to work done by others.

When my wife and I visited the Soviet Union in 1971, we spent on unforgettable day at a dacha outside Moscow, where we met Sergei's wife and children. She had prepared a wonderful meal with homemade kvas. Later in the day we met Akhmanov's mother, a professor of English literature. She insisted that we have another dinner with her as well. Our deepest sympathy goes to these surviving family members.

The last times Sergei and I got together was at the IQEC 12, held in 1989 in New Hampshire, and at a binational conference on spectroscopy of condensed matter, held in Irvine, California, in January 1990. Sergei talked about diverse topics, which, as usual, were close to my own scientific interests. They included second-harmonic generation by quadrupolar interactions in metallic single crystals, femtosecond pulse interactions in gallium arsenide, and chaotic transitions in two-dimensional multimode laser patterns. This is not the place to enumerate all of his scientific accomplishments, which one may find in his bibliography, but we may mention that Professor S A Akhmanov occupied the Chair of General Physics and Wave Processes at Moscow State University from 1975. There he established and chaired the International Laser Center of the Central and East European countries. He was Vice-Chairman of the Council on Coherent and Non-linear Optics of the USSR Academy of Sciences. He also received the Lomonosov Prize. He served on organizing and program committees of various international scientific conferences.

This volume attests to the high esteem in which he was held by many colleagues in the Western scientific establishment. We all say farewell to a scientist and friend.

N Bloembergen

Harvard University
Cambridge, Massachusetts, December 1991

CONTENTS

SECTION III NEW DEVICES AND TECHNOLOGY

Channelling of atoms in a standing laser light wave

V I Balykin†, V S Letokhov and Yu B Ovchinnikov

Institute of Spectroscopy, Russian Academy of Sciences, 142092 Troitsk, Moscow Region, Russia

1. Introduction

The effect of laser fields on the mechanical motion of atoms has recently been the subject of extensive studies of atomic physics (see reviews [1–5], special issues of scientific journals [6, 7], monographs [8, 9], and conference proceedings [10]).

Of special interest here is the interaction between atoms and a standing light wave—one of the simplest monochromatic light field configurations. Two interaction modes are possible in that case. The first occurs when the atoms are scattered by the light wave (see review [1]) and usually presupposes the fulfilment of the condition $kv_z < \tau^{-1}$, where $k = 2\pi/\lambda$ is the wave number, v_z is the atomic velocity component directed along the standing light wave, and τ is the time of flight of the atoms through the wave. This condition means that the atoms, while flying through the light wave, have enough time to move a distance of $\Delta z \simeq v_z\tau \leq \lambda/2\pi$ along it. In the second case where $kv_z \gg \tau^{-1}$, there may take place the channelling or one-dimensional trapping (localization) of the atoms.

The idea of atomic channelling, based on the classical atom-standing-light-wave interaction concept, was set forth in [12] the authors of which suggested that the effect should be used to eliminate the Doppler broadening of spectral lines.

This paper reviews the investigations performed at the Institute of Spectroscopy into this non-linear optic effect.

2. Gradient force and atomic potential for a standing light wave

Let us consider the interaction between a two-level atom and a quasi-resonant monochromatic standing wave of the form

$$\boldsymbol{E} = \hat{\boldsymbol{e}}\, 2E_0 \cos(\omega t)\cos(kz) \tag{1}$$

where E_0 is the amplitude of the travelling light wave forming the standing wave.

So that we can consider classically the motion of an atom in such a standing light wave, the following condition must be satisfied:

$$p_z \gg \hbar k \tag{2}$$

where $p_z = Mv_z$ is the atomic momentum component directed along the standing wave. Assuming that $\Delta p_z < p_z$, which is reasonable enough, one can clearly see that it

† Presently at the University of Konstanz, D-7750, Konstanz, Federal Republic of Germany.

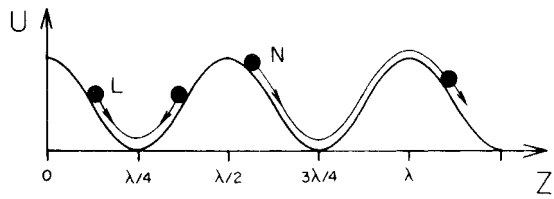

Figure 1. Atomic localization in a plane standing light wave. L denotes a localized atom oscillating near the bottom of a potential well and N a non-localized atom.

is only in this case that, according to the uncertainty principle, the uncertainty Δz of the atomic z-coordinate is less than the optical wavelength λ. Assume that the upper bound on the z-component of the atomic velocity is set by the relations

$$kv_z < \gamma \tag{3a}$$

$$kv_z < \Delta^2/\gamma(G_0)^{1/2} \tag{3b}$$

where 2δ is the natural transition width of the two-level atom, $\Delta = \omega - \omega_0$ is the detuning of the laser field frequency ω with respect to the atomic transition frequency ω_0, $G_0 = d^2E_0^2/2\hbar^2\delta^2$ is the transition saturation parameter, and d is the dipole moment matrix element of the two-level atom. Inequality (3b) reflects the absence of Landau–Zener transitions [11]. Assume also that the atom–standing-light-wave interaction time satisfies the inequality $\tau \gg \delta^{-1}$.

Under the above assumptions, the motion of an atom in a standing light wave is governed by the gradient (or dipole) force

$$\boldsymbol{F}_g = -(\partial U_g/\partial z)\boldsymbol{e}_z \tag{4}$$

of potential nature. The associated potential has the form [13]

$$U_g = (\hbar\Delta/2)\ln\{1 + G/[1 + (\Delta/\gamma)^2]\} \tag{5}$$

where $G = 4G_0\cos^2(kz)$ is the atomic transition saturation parameter in the standing light wave.

In the limiting case of weak saturation and large frequency detuning,

$$G \ll 1 + (\Delta/\delta)^2 \tag{6a}$$

$$\Delta \gg \delta \tag{6b}$$

the expression for the potential U_g reduces to the simple form

$$U_g = (\hbar g_0^2/\Delta)\cos^2(kz) \tag{7}$$

where $g_0 = dE_0/2\hbar$ is the Rabi frequency and the saturation parameter $G = 2g_0^2/\gamma^2$.

Expression (7) is equivalent to the following classical relation used in [12]:

$$U_g = -\alpha E_0^2\cos^2(kz) \tag{8}$$

where α is the polarizability of the atom at the optical frequency:

$$\alpha = e^2/m(\omega_0^2 - \omega^2) = (n_\omega - 1)/2\pi N \tag{9}$$

where n_ω is the refractive index of the medium containing N atoms in a unit of volume.

It follows from expressions (5), (7) and (8) that the period of the potential U_g is equal to half the optical wavelength. When the field frequency detuning is positive ($\Delta > 0$), the potential wells coincide with the nodes of the standing light wave, and when it is negative ($\Delta < 0$), with the wave loops. Figure 1 illustrates this potential for the case $\Delta > 0$.

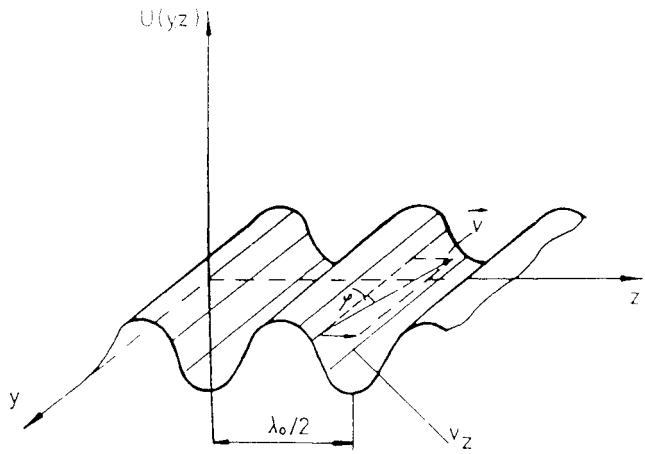

Figure 2. Potential energy of an atom in a standing light wave wherein atoms moving with a velocity of v are trapped (from [14]).

What is the character of atomic motion in such a potential? Assume that the amplitude (depth) of potential (5) is $U_g^0 \gg R$, where $R = \hbar^2 k^2/2M$ is the recoil energy acquired by the atom upon absorption of a single photon. The atoms flying through the standing light wave will in that case be divided into two groups according to their total energy $W = U(z) + Mv^2(z)/2$. The atoms with a total energy of $W < U_g^0$ will move between the adjacent potential maxima. Such atoms are referred to in the text below as localized. In the general case, the localized atoms perform anharmonic oscillations with an amplitude of less than $\lambda/4$ about the potential wells.

The atoms with a total energy of $W > U_g^0$ move infinitely along the z-axis, the potential modulating the corresponding atomic velocity component. Such atoms will be called non-localized. The classical atomic motion in a potential similar to (5) in the weak-saturation limit has been considered in detail in [14].

3. Theory of atomic motion in a standing light wave

Let us now consider atomic motion in a one-dimensional monochromatic standing wave. In that case, atoms can be localized in one direction, but will move freely in any other direction, and so they are channelled along the light wave front (figure 2). The motion of an atom here can be determined in the quasi-classical approximation by integrating the Langevin equation [15]

$$\mathrm{d}\boldsymbol{p}/\mathrm{d}t = \boldsymbol{F} \tag{10}$$

where $\boldsymbol{p}$ is the atomic momentum and $\boldsymbol{F}$ is the total force acting on the atom. The force $\boldsymbol{F}$ may be represented in the form

$$\boldsymbol{F} = \boldsymbol{F}_g + \boldsymbol{F}_{fr} + \boldsymbol{F}_d \tag{11}$$

where $\boldsymbol{F}_g$ is the gradient force, $\boldsymbol{F}_{fr}$ is that part of the total force which depends on the atomic velocity (i.e., the friction force), and $\boldsymbol{F}_d$ is the fluctuating force due to the atomic momentum diffusion.

The gradient force for the two-level atom is given by expression (5). The friction force for such an atom is [13, 16]

$$\boldsymbol{F}_{\rm fr} = 2\hbar(\Delta/\gamma)G\{[1+(\Delta/\gamma)^2 - G(1+G/2)]/[1+(\Delta/\gamma)^2+G]^3\}\tan^2(\boldsymbol{k}\cdot\boldsymbol{z})\boldsymbol{k}(\boldsymbol{v}\cdot\boldsymbol{k}). \tag{12}$$

Besides, allowing for the quantum absorption and emission of photons by the atom causes the radiative force to fluctuate about its mean value. According to [13, 17], the atomic momentum diffusion coefficient, $2D = \langle\Delta p^2\rangle/\Delta t$, which characterizes the build-up rate of the mean-square atomic momentum fluctuation about its mean value, is defined by the relations

$$2D_{\rm i} = \hbar^2k^2\gamma G(\{[1+(\Delta/\gamma)^2]^2 + [3-(\Delta/\gamma)^2]G + 3G^2 + G^3\} \times [1+(\Delta/\gamma)^2+G]^3)\tan(\boldsymbol{k}\cdot\boldsymbol{z}) \tag{13a}$$

$$2D_{\rm sp} = \hbar^2k^2\gamma\{G/[1+(\Delta/\gamma)^2+G]\} \tag{13b}$$

where $2D_{\rm i}$ stands for the atomic momentum diffusion due to the induced emission and absorption of photons and $2D_{\rm sp}$ denotes that due to the spontaneous emission of photons.

Let us analyse briefly the above expressions. First of all, it should be noted that the motion of an atom in a standing light wave is, on the whole, determined by the three factors considered above. The motion of a single atom in a standing light wave is described by the Langevin equation given by (10) and (11), wherein $\boldsymbol{F}_{\rm d}$ is the random Langevin force, zero on average, whose fluctuations are governed by the atomic momentum fluctuations depending on the diffusion coefficient defined by (13*a*) and (13*b*) [15]. Note that the part of this force which is due to induced atomic momentum fluctuations is directed along the light-field gradient, while its other part, the one due to spontaneous transitions, has a random direction varying with a frequency equal to the rate of these transitions. Whereas the random force can, on average, only heat the atom, the friction force can both heat and cool it. As seen from (12), the friction force changes sign when $1+(\Delta/\delta)^2 = G(1+G/2)$. We would like to consider the situation where the friction force is directed against the atomic velocity, i.e., where it cools the atom and causes it to be localized in the vicinity of the potential well (5). Two cases can be distinguished here.

(a) 'Red shift' case

$$\Delta < 0 \qquad 1+(\Delta/\gamma)^2 > \overline{G(1+G/2)}. \tag{14}$$

The friction force in this case reaches its maximum, which does not exceed the maximum of the spontaneous light pressure force, $F_{\rm sp}^{\rm max} = \hbar k\delta$, at $\Delta \simeq \delta$ and $G \simeq 1$. The atomic momentum diffusion coefficient here is $2D \simeq \hbar^2k^2\delta$, and the potential depth is not very great, $U_{\rm g}^0 \simeq \hbar\delta$. The time for which the atom can be held localized within the limits of a potential well $\lambda/2$ in size (figure 1) can be taken to be approximately equal to that required for it to acquire, as a result of momentum diffusion, an energy equal to the depth of the well, i.e., $\tau_0 \simeq U_{\rm g}^0$, $M/D \simeq 1/kv_{\rm r} = 10^{-6}$ s, where $v_{\rm r} = \hbar k/M$ is the recoil velocity. This rough estimate agrees well with the more stringent estimate made in [18]. By increasing the frequency detuning and the intensity of the standing-light-wave field one can lengthen the atomic confinement time but cannot make the potential depth greater than $U_{\rm g}^0 \simeq \hbar\delta$ under the condition

$$1+(\Delta/\delta)^2 > \overline{G(1+G/2)}.$$

If this condition is not satisfied, the friction force changes sign, which leads to an additional heating of the atom.

It was precisely the 'red shift' case that was originally proposed to localize atoms in a three-dimensional standing light wave [19, 20].

(b) 'Blue shift' case:

$$\Delta > 0 \qquad 1 + (\Delta/\gamma)^2 < \overline{G(1 + G/2)} \tag{15}$$

In contrast to the preceding case, one can achieve, with the parameters given above and $\Delta \gg \delta$, comparatively high potential depth and friction force values, $U_g^0 \simeq \hbar\Delta$ and $\boldsymbol{F}_{fr} \simeq \hbar\boldsymbol{k}\Delta v$. On the other hand, the induced momentum diffusion coefficient in the case of strong light fields becomes much greater than its spontaneous counterpart: $2D_i \simeq \hbar^2 k^2 \delta G$. What is more, the analysis of this situation is more difficult to make, both the friction force and atomic momentum diffusion being strong functions of space. Figure 3 shows the spatial dependences (in the space interval 2λ) of the potential U_g, the friction coefficient $\beta(\boldsymbol{F}_{fr} = -\beta v)$ and the atomic momentum diffusion coefficient $2D = 2D_i + 2D_{sp}$ for a saturation parameter of $G_0 = 10^4$ and three different frequency detuning values: $\Delta = 20\delta$, 100δ and 500δ. As can be seen from figure 3(a), the potential reaches its maximum at an optimum frequency detuning of $\Delta_{opt} \simeq 2\delta(G_0)^{1/2} = 100\delta$. The efficiency of cooling atoms by the friction force can be estimated by means of the parameter $\chi = \beta/2D$.

It has been demonstrated in the theoretical works reported in [21, 22] that the quantity $1/\chi$ represents the temperature of the atoms in the standing light wave, provided their energy $W \gg U_g^0$, for it is only in this case that the atomic energy obeys the Boltzmann distribution law. One can see from expressions (12) and (13a) and from figures 3(b), 3(c) and 4 that reducing the frequency detuning will increase χ but narrow at the same time the range $2z_0$ of non-zero χ values in the vicinity of the standing-wave nodes. To illustrate, for $\Delta = 20\delta$, $\chi \simeq 0.15(\hbar\delta)^{-1}$ and $z_0 \simeq 10^{-2}\lambda$; for $\Delta = 100\delta$, $\chi \simeq 0.1\ (\hbar\delta)^{-1}$ and $z_0 \simeq 2 \times 10^{-2}\lambda$; and for $\Delta = 500\delta$, $\chi \simeq 0.06\ (\hbar\delta)^{-1}$ and $z_0 \simeq 6 \times 10^{-2}\lambda$.

The time for which an atom can be localized in a potential well of the standing light wave is $\tau_0 \simeq (\Delta/\delta)^{2/3}/kv_r$ [22]. For $\Delta = 10^3\delta$, this time may be of the order of a few milliseconds. On the other hand, it is highly probable that once the atom has escaped from the well it will be trapped again in another one [22]. The atomic motion thus resembles the Brownian wandering across the individual potential wells produced by the standing light wave. The characteristic lifetime of the atom in each of the wells is of the order of τ_0. Such behaviour of the atom is corroborated by the analysis of the experimental results reported in [15].

As for the spatial distribution of the atoms with an energy of $W < U_g^0 \simeq \hbar\Delta$, most of them are concentrated in regions with a characteristic size of $z_0^* \simeq (\delta/\Delta)^{1/3}/k$ near the standing-wave nodes [22]. Thus, the atomic ensemble in the standing light wave forms a lattice with period $\lambda/2$ that follows the intensity distribution period of the light field.

Let us now consider two-dimensional atomic motion in a spherical standing light wave formed by a laser beam with a Gaussian intensity distribution. Suppose that the standing wave is crossed by an atomic beam. At a certain point in the wave where the transverse kinetic energy of the atoms is equal to their potential energy in the light field, they can be localized in a potential well. The atoms will then be channelled along the nodes (or loops) of the wave, for their trajectories must follow the wave front accurate to within less than λ. Figure 5 illustrates the behaviour of the

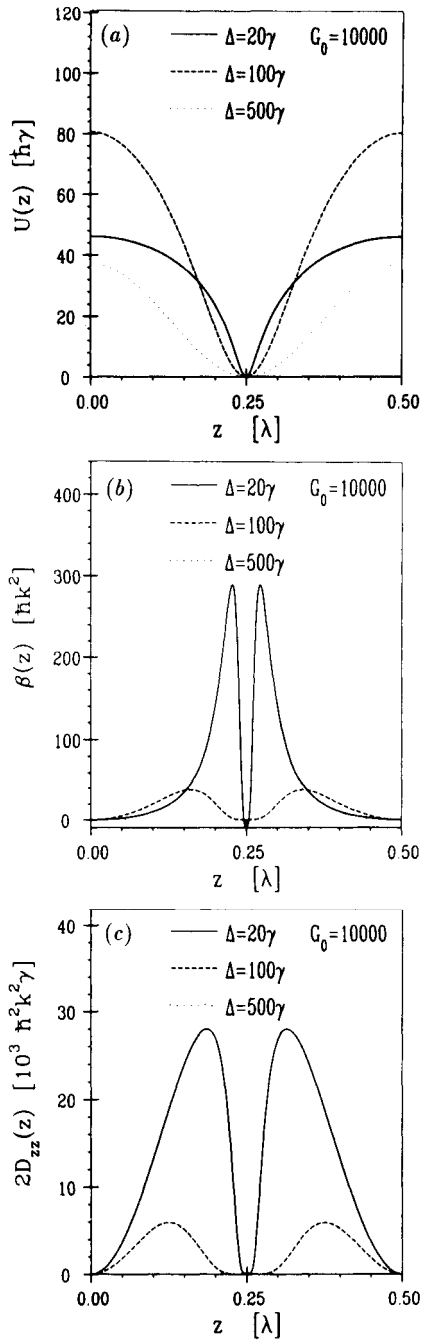

Figure 3. Spatial behaviour of (*a*) the atomic potential energy, (*b*) the friction coefficient, and (*c*) the atomic momentum diffusion in a standing light wave.

potential energy of (1) localized and (2) non-localized atoms in the spherical standing light wave, which reflects their trajectories in the laser field. The atoms, spaced a

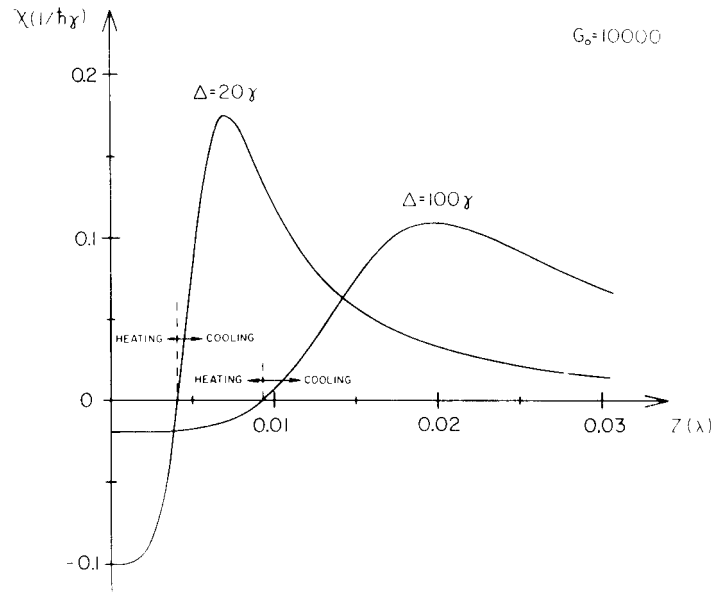

Figure 4. Spatial dependence of the parameter χ near a standing light-wave node.

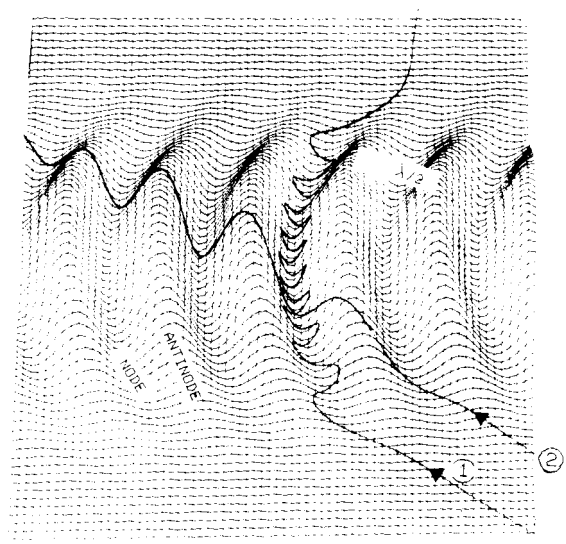

Figure 5. Atomic potential energy in a spherical standing light wave for (1) localized atoms and (2) non-localized ones. The curves reflect the trajectories of the localized and non-localized atoms.

distance of $d = \lambda/2$ apart, move parallel to one another and enter the field near the minimum of two adjacent potential wells. The laser field parameters are as follows: the laser power $P = 0.11$ W, the frequency detuning $\Delta = 400$ MHz, and the radius of curvature of the wave front, $R = 2$ m. The atoms differ in longitudinal velocity,

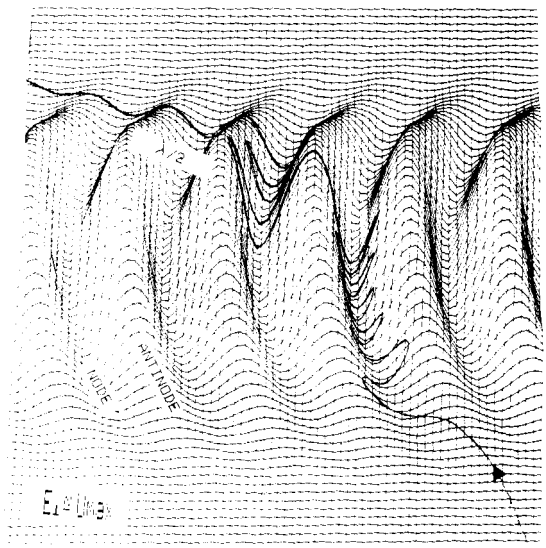

Figure 6. Effect of atomic momentum diffusion on the motion of atoms. The transverse kinetic energy of the atoms is a little lower than the potential maximum. The momentum diffusion raises this energy so that it becomes higher than the maximum potential energy at a certain point in the standing light wave, which prevents the atoms from being localized.

the localized atoms moving with a velocity of $v = 500$ m s^{-1} and their non-localized counterparts with a velocity of $v = 1200$ m s^{-1}. The atoms moving with the higher velocity will have, at a certain point in the field, their transverse kinetic energy higher than the potential maximum, and so will fly on freely.

Figure 6 shows the effect of momentum diffusion on the motion of atoms. The transverse kinetic energy of the atoms is a little lower than the potential maximum. The atomic momentum diffusion raises the kinetic energy so that it becomes, at some point in the standing light wave, higher than the potential maximum, and the atoms are thus prevented from being localized.

When the atomic transition saturation parameter is much less than unity and the atom–light-field interaction time is such that the change in the atomic momentum due to friction and diffusion is insignificant, both the friction force and atomic momentum diffusion can be disregarded. In that case, the atom sees the light wave as a spatially periodic potential field whose period is equal to that of the spatial light-field intensity distribution.

Figure 7 illustrates the change in the transverse velocity of the localized atoms in the course of their flight through the spherical standing light wave, calculated by equations (10) and (11). The atomic motion calculations have been made with and without the friction force being taken into consideration. The non-localized atoms receive a push in the region where their trajectories are tangent to the standing wave front. The friction force changes the atomic oscillation amplitude but has no effect on the character of atomic motion.

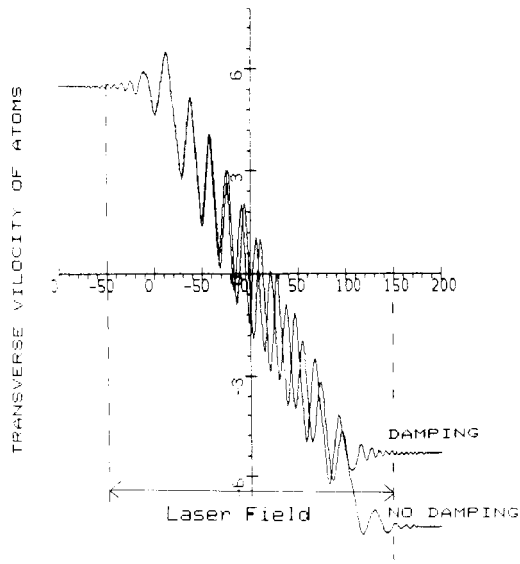

Figure 7. Transverse velocity variation of atoms localized in a spherical standing light wave in the course of their flight.

4. Experimental observation of the channelling of atoms

One of the manifestations of the atomic channelling effect in a standing light wave is the concentration of atoms near the nodes ($\Delta > 0$) or loops ($\Delta < 0$) of the wave. The first experiments in this field were aimed at detecting such spatial redistribution of atoms in a standing light wave. For example, the authors of [23] measured the fluorescence signal from an atomic beam intersecting a standing light wave at right angles. This signal was found to depend asymmetrically on the frequency detuning of the wave. These investigators attributed this asymmetry to the redistribution of atomic density in the standing wave potential produced by the gradient force. They believed that at negative frequency detunings the atoms concentrated near the loops of the standing wave. i.e., in regions where the field intensity was high, which resulted in an increased fluorescence signal, whereas at positive detunings, the atoms concentrated near the standing wave nodes, and the fluorescence signal thus decreased.

The distribution of atoms in a standing light wave was studied in more detail in [24]. The authors of this work measured the frequency dependence of the coefficient of absorption of an auxiliary weak probe wave passing through the region where an atomic beam cut across a strong standing light wave. As a result of the optical Stark shift, the frequency at which an atom absorbs the probe radiation depends on the light-field intensity at its location in the standing wave. The spatial distribution of atoms in a standing light wave can be estimated by analysing their absorption line profiles. This experiment also demonstrated that the atom concentrated in the vicinity of the standing wave nodes at $\Delta > 0$, and near the loops at $\Delta < 0$.

A number of experiments were staged to measure the changes in the microscopic atomic motion parameters following the atom–standing-light-wave interaction. The simplest experiment of this kind [25, 26] involved the scattering of atoms by the potential of a standing light wave (figure 8(*a*)). In these experiments, both the

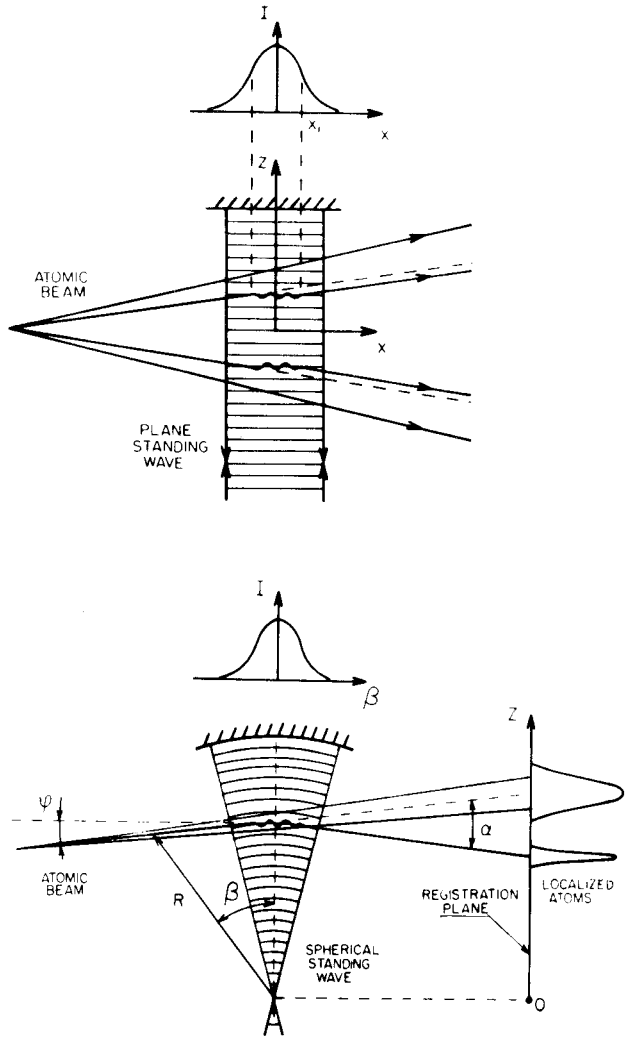

Figure 8. Localization of atoms in (*a*) a plane standing light wave (top—light-field intensity distribution along the transverse coordinate of the laser beam forming the standing wave) and (*b*) a spherical standing light wave.

divergence and shape of the atomic beam changed. These changes, however, do not allow one to speak with assurance about such details of channelling as the proportion of localized atoms and their confinement time in the potential wells.

The situation is quite different where the atomic beam interacts with a spherical standing light wave [15, 27, 28]. The experiment is illustrated schematically in figure 8(*b*). The spherical standing light wave is formed by a laser beam (with a Gaussian transverse intensity distribution) reflecting from a spherical mirror. The laser field is monochromatic, and its frequency detuning $\Delta > 0$. A beam of Na atoms meets the standing light wave tangentially to its front. The atoms localized in the

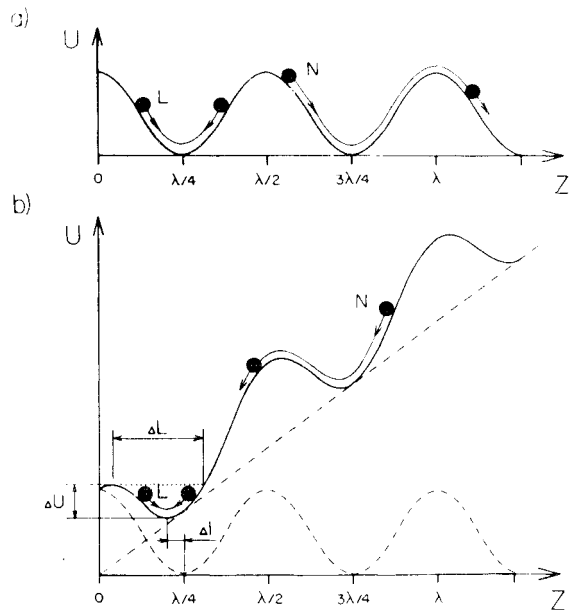

Figure 9. Effective potential for atoms in a spherical standing light wave. The centrifugal force displaces the bottom of the potential well (Δ/l) and reduces its width (ΔL) and depth (Δu).

standing wave (i.e., ones entering the wave near its potential minima) move on along the potential wells whose bend is similar to that of the nodal surfaces of the wave. As a result, the localized atoms are deflected through an angle of θ from their initial direction, θ being the angular divergence of the standing light wave. Disregarding the effect of the friction force, the non-localized atoms can be said to suffer only scattering in the standing light wave and gather a characteristic transverse velocity of $v_{cr} = (2U_g^0/M)^{1/2}$ determined by the amplitude of the standing wave potential U_g^0. So, for a beam of thermal atoms with a small angular divergence of $\Delta\varphi < \theta/2$, it is not very difficult to find such standing light wave parameters (θ, Δ, G) as will make the beam of localized atoms diverge from that of their non-localized counterparts.

Let us now consider the conditions necessary to localize atoms in a spherical standing light wave, and also some specific features of atomic localization in a plane standing light wave.

We will analyse the motion of an atom in a region within the standing light wave, the size of which is much smaller than the radius R of the light wave curvature in this region. If, in addition, the condition $v \gg v_{cr}$ is valid for the atomic velocity, we can assume that in the polar coordinate system associated with the light wave (figure 8(b)), the atom is acted upon by the constant centrifugal force $F_{cf} = Mv_t^2/R$, where v_t is the tangential atomic velocity component. The atomic motion in this coordinate system is governed by the effective potential $U_{eff} = U_g + F_{cf}R$ (figure 9). It can be seen from this figure that the centrifugal force reduces the size of the potential wells, displaces them along the standing light wave, and reduces the potential depth down to $\Delta U = U_g^0 - F_{cf}(\lambda/4)$, provided that $F_{cf} \ll F_g^{max} = \sup(-\partial U_g/\partial R)$. On the other hand, these potential wells can only exist if $F_g^{max} > F_{cf}$.

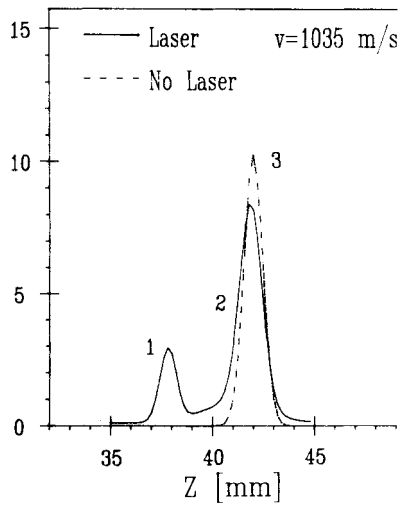

Figure 10. Experimental transverse profile of an atomic beam following its interaction with a spherical standing light wave. Peak 1 corresponds to the atoms localized in the wave and peak 2, to non-localized atoms. Dashed curve 3 corresponds to no-laser-field conditions.

An atom can be localized in a spherical standing light wave only if its radial velocity component v_R satisfies the inequality $Mv_R^2/2 < \Delta U$. This occurs in the vicinity of the point where the atomic trajectory is conjugate to the standing wave, $\beta = \varphi$ and $v_R = 0$ in the absence of the wave. The characteristic size of this region is $L \simeq (R/v)(2\Delta u/M)^{1/2}$. In the case of the $3^2S_{1/2} \rightarrow 3^2P_{3/2}$ transition in Na ($\delta = 3 \times 10^{-7}$ s^{-1}, $M = 4 \times 10^{-23}$ g) at $\Delta U = 10\hbar\delta \simeq 3 \times 10^{-19}$ erg, $v = 10^5$ cm s^{-1}, and $R = 1$ cm, the size $L \simeq 10^{-3}$ cm, i.e., the place of possible localization of the atom has been correctly determined to be the tangency point with the coordinates φ and R.

The analysis of the motion of an atom in the potential presented in figure 9 shows that the most favourable conditions for the atom to be localized occur when the atomic trajectory coincides with the curvature of standing light wave at its edge, where $F_g \simeq F_{cf}$. In the case of weak saturation, a 100% localization can be achieved if the transverse potential gradient satisfies the following conditions in the vicinity of the localization point:

$$\partial U/\partial p = F_\perp \geq (F_{cf}/2)(v_{cr}^*/v) \tag{16}$$

where $v_{cr}^* = (F_{cf}\lambda/M)^{1/2}$. This expression holds true where the contribution from the diffusion of atoms in the course of channelling is small, i.e., where $\partial U/\partial p > D/Mv$.

Consequently, two conditions must be satisfied for atoms to become localized in a spherical standing light wave. First, condition (16) must be fulfilled at the tangency point. Secondly, the potential in the vicinity of this point must obviously grow higher in the direction of atomic motion. In other words, this point must be located at the entrance half of the wave.

Figure 10 illustrates the characteristic atomic beam intensity distribution in a plane 290 mm distant from the standing light wave. The wave was formed by a single-frequency laser beam detuned by an amount of $\Delta/2\pi = 90$ MHz from the frequency of the $3^2S_{1/2}(F = 2) \rightarrow 3^2P_{3/2}(F' = 3)$ transition in Na, the laser beam intensity in the atom–laser-field interaction region being $I = 20$ W cm^{-2}. The waist of the laser

beam in the interaction region was $2W = 0.6$ mm (with reference to the I/e^2 intensity level), its angular divergence θ amounting to 1.5×10^{-2} rad. The atomic beam had an angular divergence of $\Delta\varphi = 3 \times 10^{-3}$ rad and intersected the laser beam at an angle of $\varphi = 7 \times 10^{-3}$ rad. As can be seen from figure 10, the distance between the atomic beam intensity peaks is $\Delta z = 4.3$ mm, which corresponds to a deflection angle of the localized atoms of $\alpha_{\text{eff}} \simeq 1.5 \times 10^{-2}$ rad. This angle agrees well with the predicted value $\alpha = \theta = 1.5 \times 10^{-2}$ rad.

For our experiment, expression (16) is invalid. As a result, it was only about 30% of the atoms incident upon the spherical standing light wave that got localized in it (figure 10). Besides, our experimental results allowed us to conclude that all the atoms forming peak 1 in the detection zone moved in the standing light wave along certain potential wells without any jumps between them. So, the characteristic lifetime of the atoms in individual wells exceeded their time of flight through the wave, $\tau \simeq 1$ μs.

As seen from figure 9, the probability of the atoms jumping from one potential well into another in the spherical standing light wave is low. If an atom escapes from a potential well, it already possesses an energy of the order of $F_{\text{cf}}\lambda/4$ by the time it reaches the next well. With $F_{\text{cf}} \simeq F_{\text{g}}$, the centrifugal acceleration of the atom reduces its probability of being localized again. Quite a number of technical factors prevented one from attaining times of flight of the atoms through the standing light wave longer than 1 μs in the experiments reported in [15, 28]. If, however, longer times of flight are achieved, it will be possible to measure directly the confinement times of atoms in individual potential wells. It should be noted that these times differ from the confinement time in a plane standing light wave [22]. This is mainly due to the bottoms of the effective potential wells in the spherical standing light wave being displaced relative to its nodal lines (figure 9), with the result that neither diffusion coefficient (13), nor friction force (12) goes to zero at the bottom of the effective potential wells.

5. Collimation of an atomic beam by way of atomic channelling

An atom can be localized in a spherical standing light wave if its trajectory is tangent to the wave front at the entrance point, the gradient force exceeds the centrifugal force, and the field intensity grows higher in the direction of atomic motion. In the course of localization, the longitudinal atomic velocity is transformed into transverse velocity. If the law governing the light-field intensity distribution differs between the entrance and exit edges of the wave, the transverse atomic velocity at the exit from the wave may differ from its initial value, i.e., there may occur an effective transverse cooling of the atoms [29]. The relative transverse cooling of the atomic beam is defined by the relation [29]

$$T_{\text{f}}/T_{\text{in}} = (4e^2/\pi)(R\lambda/W^2) \tag{17}$$

which contains only the geometrical parameters of the standing light wave at the point of its intersection with the atomic beam, namely, its radius of curvature R and the laser beam radius W. Figure 11 illustrates schematically the transverse cooling of atoms by way of their channelling in a truncated spherical standing light wave. The wave was formed by shutting half the beam of a single-frequency cw laser with a safety razor blade. The spatial profile of the laser beam is shown at the top of the figure. The transverse cooling of the atoms was detected by measuring the spatial profiles of the atomic beam following its intersection with the standing light wave.

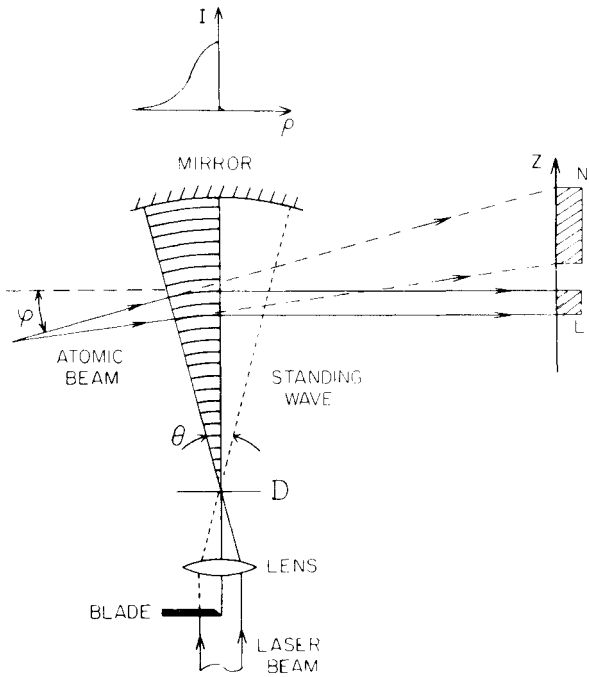

Figure 11. Transverse cooling of atoms by way of their channelling in a truncated spherical standing light wave. The wave was formed by shutting half the beam of a single-frequency CW laser with a safety razor blade. Top—spatial laser beam profiles.

Figure 12 presents the results of such measurements. The solid curve corresponds to the whole spherical standing light wave, and the dashed one, to the truncated wave. Peak 1 is produced by the atoms localized in the whole wave, peak 2 is formed by the atoms localized in the truncated wave, and peak 3 is due to the non-localized atoms. Peak 2 due to the atoms localized in the truncated wave is narrower than the peak produced by the non-localized atoms. The transverse atomic temperature in this experiment was reduced from $k_B T_{in} = 8.5\hbar\delta$ to $k_B T_f = 2.1\hbar\delta$. The numerical modelling of the experiment yielded a value of $1.3\hbar\delta$ for the final atomic temperature $k_B T_f$, which was in good agreement with the experimental value.

6. Conclusion

A natural extension of the atomic channelling effect, i.e., one-dimensional localization, is the channelling of atoms in two (two-dimensional localization) and three (three-dimensional localization) standing light waves intersecting at right angles. In the latter case, which was already considered in [14, 20], atoms can be trapped in small regions less than $\lambda/2$ in size. The localization of an atom in a three-dimensional standing light wave in the case of red shift, $\Delta \simeq -\delta$, was observed in [30]. Based on the fact that the measured width of the elastic component of the fluorescence spectrum was $\Delta\nu \simeq$ 70 kHz, the confinement time τ of the atom in a potential well was estimated at 2.3 μs. This value agrees well with that given in section 2 for the case of red shift.

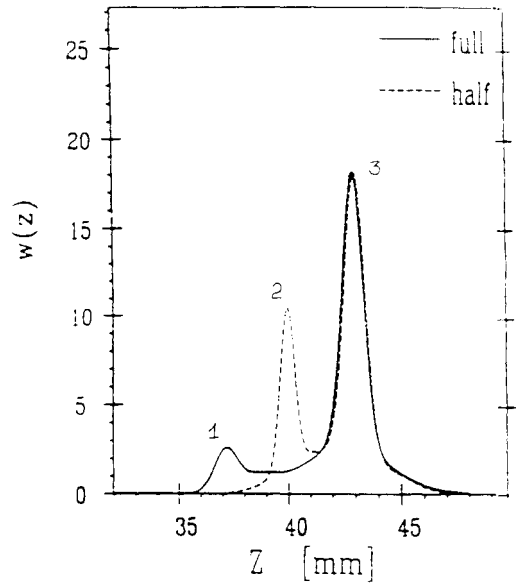

Figure 12. Experimental results of the transverse cooling of atoms by way of channelling. The solid curve corresponds to the whole spherical standing light wave and the dashed one, to the truncated wave. Peak 1 is produced by the atoms localized in the whole wave, peak 2 is formed by the atoms localized in the truncated wave, and peak 3 is due to the non-localized atoms.

This opens up a number of interesting application possibilities. First, the Doppler broadening is eliminated for all the spectral lines of localized atoms (Lamb–Dicke regime), and it was this application of the channelling effect that was proposed in [12]. Secondly, three-dimensional localization gives rise to a regular, spatially periodic arrangement of the absorbing and emitting atomic particles. In that case, it might be expected that absorption and emission anisotropy effects will become manifest similar to the Bragg diffraction.

References

[1] Ashkin A 1980 *Science* **210** 1081
[2] Letokhov V S and Minogin V G 1981 *Phys. Rep.* **73** 1
[3] Stenholm S 1986 *Rev. Mod. Phys.* **58** 699
[4] Phillips D, Gould P I and Lett P D 1991 *Science* **239** 878
[5] Cohen-Tannoudji C 1991 *Fundamental Systems in Quantum Optics* (Elsevier Science Publ. BV)
[6] Meystre P and Stenholm S (ed) 1985 *J. Opt. Soc. Am.* B **5** 11
[7] Chu S and Wieman C (ed) 1990 *J. Opt. Soc. Am.* B **6** 2109–278
[8] Minogin V G and Letokhov V S 1978 *Laser Light Pressure on Atoms* (New York: Gordon & Breach)
[9] Kazantsev A P, Surdutovich G I and Yakovlev V P 1991 *Mechanical Action of Light on Atoms* (Singapore: World Scientific)

[10] Moi L, Gozzini S, Gabbanini C, Arimondo E and Strumia F (ed) 1991 *Light Induced Kinetic Effects* (Piza: ETS Editrice)
[11] Kazantsev A P, Ryabenko G A, Surdutovich G I and Yakovlev V P 1985 *Phys. Rep.* **129** 75
[12] Letokhov V S 1968 *Pis'ma Zh. Eksp. Teor. Fiz.* **7** 348 (Engl. Trans. 1968 *Sov. Phys.-JETP Lett.* **7** 272)
[13] Gordon J P and Ashkin A 1980 *Phys. Rev.* A **21** 1606
[14] Letokhov V S and Pavlik B D 1976 *Appl. Phys.* **9** 229
[15] Balykin V I, Lozovik Yu E, Ovchinikov Yu B, Sidorov A I, Shul'ga S V and Letokhov V S 1989 *JOSA* B **6** 2178
[16] Kazantsev A P, Chudesnikov D O and Yakovlev V P 1986 *Zh. Eksp. Teor. Fiz.* **63** 951 (in Russian)
[17] Cook R J 1980 *Phys. Rev.* A **22** 1078
[18] Baklanov E V 1987 *Pis'ma Zh. Eksp. Teor. Fiz.* **45** 247 (in Russian)
[19] Letokhov V S 1975 *Science* **190** 344
[20] Letokhov V S, Minogin V G and Pavlik B D 1976 *Opt. Commun.* **19** 72; 1977 *Zh. Eksp. Teor. Fiz.* **72** 1328 (in Russian)
[21] Kazantsev A P, Smirnov V S, Surdutovich G I, Chudesnikov D O and Yakovlev V P 1985 *JOSA* B **2** 1731
[22] Kazantsev A P, Surdutovich G I and Yakovlev V P 1988 *Opt. Commun.* **68** 103
[23] Prentiss M G and Ezekiel S 1986 *Phys. Rev. Lett.* **56** 46
[24] Salamon C, Dalibard J, Aspect A, Metcalf H and Cohen-Tannoudji C 1987 *Phys. Rev. Lett.* **59** 1659
[25] Arimondo E, Lew H and Oka T 1987 *Phys. Rev. Lett.* **43** 753
[26] Tauguy C, Reynaud S and Cohen-Tannoudji C 1984 *J. Phys. B: At. Mol. Phys.* **17** 4623
[27] Cloppenpurg K, Henning G, Mihm A, Wallis H and Ertmer W 1987 *Laser Spectroscopy VIII* (Berlin: Springer) p 87
[28] Balykin V I, Letokhov V S, Ovchinnikov Yu B, Sidorov A I and Shul'ga S V 1988 *Opt. Lett.* **13** 958
[29] Balykin V I, Letokhov V S, Ovchinnikov Yu B and Shul'ga S V 1990 *Opt. Commun.* **77** 152
[30] Westbrook C I, Watts R N, Tanner C E, Rolston S L, Phillips W D, Lett P D and Gould P I 1990 *Phys. Rev. Lett.* **65** 33

Optical nonlinearities and the Kerr-effect in phaseonium

U. Rathe,[a] M. Fleischhauer,[a,b] and Marlan O. Scully[a,b]

[a]Center for Advanced Studies and
Department of Physics and Astronomy
University of New Mexico
Albuquerque, New Mexico 87131

and

[b]Max-Planck Institut für Quantenoptik
D-8046 Garching
Federal Republic of Germany

Recent studies have shown that three-level atoms having a ground (excited) state doublet connected to an excited (ground) state via an optical frequency transition can display unusual behavior when the doublet is coherently prepared. Such a phased ensemble of atoms (phaseonium) is in a very real sense a new state of matter. For example, such a medium can display cancellation of optical absorption while at the same time retaining emission from the excited state to the ground state doublet (lasing without inversion). It has recently been shown that it is, in principle, possible to have a condition in which there is an enhancement of the linear index of refraction with vanishing absorption. In this chapter, we wish to show that phaseonium can display a large nonlinear Kerr-effect near the atomic resonance while retaining complete transparency.

1 Introduction

Systems with atomic coherence can have interesting optical properties, such as non-absorbing resonances (Alzetta et al. 1976, 1978, 1979; Gray et al. 1979; Harris 1989; Imamoğlu et al. 1989a, 1989b) or an index of refraction at a frequency of vanishing absorption many orders of magnitude larger than is otherwise possible (Scully et al. 1991, 1992; Fleischhauer et al. 1992). In the following we show that such a medium can display an ultra large Kerr-coefficient near the atomic resonance while remaining completely transparent.

Near resonance nonlinearities are usually accompanied by a large absorption of the medium. By using atomic coherence effects this absorption can be cancelled while maintaining substantial values of the nonlinear susceptibilities. In a three-level system for example (see figure 1), a strong microwave driving field coupling the two closely spaced upper levels can lead to a non-absorbing resonance with a large susceptibility $\chi^{(3)}(\omega;\omega_1,\omega_2,\nu_\mu)$, corresponding to a sum-frequency generation of two optical frequencies ω_1 and ω_2 and the

* Dedicated to Academician Akhmanov who made so many enduring contributions to our understanding of nonlinear optical physics.

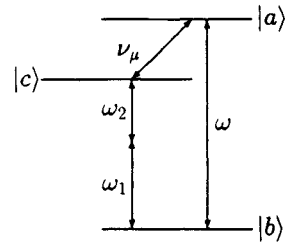

Figure 1: Level scheme for the sum-frequency generation discussed by Harris et al. (1990).

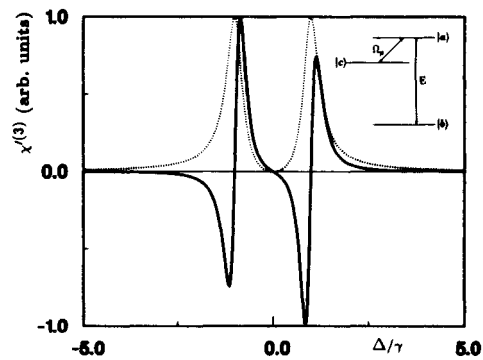

Figure 2: $\chi'^{(3)}(\omega;\omega,\omega,-\omega)$ in arbitrary units for a three-level system with a strong coherent driving field between the upper two levels as a function of the detuning (solid curve). The dotted curve shows the imaginary part of the linear susceptibility.

microwave frequency ν_μ if ω is resonant with the $|a\rangle \rightarrow |b\rangle$ transition (Harris et al. 1990; Hahn et al. 1990).

Without population in the excited state of the optical transition, however, all susceptibilities $\chi^{nl}(\omega;\pm\omega,\pm\omega,\ldots)$ containing only *one* optical frequency ω, and hence all related quantities like the Kerr-coefficient, vanish at the point of absorption cancellation as shown in figure 2. On the other hand, providing there is a small population in the upper level, the real part of the linear and nonlinear susceptibilities $\chi^{nl}(\omega;\pm\omega,\pm\omega,\ldots)$ can reach substantial values.

In the following we concentrate on one of the several proposed coherence-establishing schemes (Scully et al. 1991, 1992; Fleischhauer et al. 1992), namely the case of a three-level

atom in which an initially prepared atomic coherence between a ground-state doublet, $|b\rangle$ and $|b'\rangle$, generates a point of zero absorption and a high index of refraction for the transition to an excited state, $|a\rangle$. We compare the Kerr-coefficient for this system to that of usual Kerr-type materials such as CS_2.

2 Two-level atoms

It is well known that high nonlinearities occur near atomic resonances. To illustrate this and to make a comparison to the three-level atom with an initially prepared coherence discussed in the following section, we briefly review the text-book results for a two-level system (Sargent et al. 1974).

We consider a system of two-level atoms interacting with an electric field as shown in figure 3. The atoms are initially prepared in a mixture of states described by a diagonal density matrix ρ^0. The equations of motion for the density matrix of the ith atom in a rotating frame are

$$\dot{\rho}^i_{aa} = -\gamma_a \rho^i_{aa} - \frac{i}{\hbar}\left(\wp E \rho^i_{ba} - c.c.\right), \tag{1}$$

$$\dot{\rho}^i_{bb} = -\gamma_b \rho^i_{bb} - \frac{i}{\hbar}\left(\wp E^* \rho^i_{ab} - c.c.\right), \tag{2}$$

$$\dot{\rho}^i_{ab} = -\left(\gamma_{ab} + i\Delta_{ab}\right)\rho^i_{ab} - \frac{i}{\hbar}\wp E\left(\rho^i_{bb} - \rho^i_{aa}\right), \tag{3}$$

where E is the slowly varying amplitude of the optical probe-field, $\wp$ is the dipole-matrix element of the transition $|b\rangle \rightarrow |a\rangle$, $\Delta_{ab} = \omega_{ab} - \nu$ with ν being the frequency of the optical probe, γ_a and γ_b are the longitudinal decay rates from the levels $|a\rangle$ and $|b\rangle$ to some other levels, and $\gamma_{ab} = (\gamma_a + \gamma_b)/2$. We have assumed that the decay rate from $|a\rangle$ to $|b\rangle$ is much smaller than γ_a and γ_b and can be neglected together with decay due to collisions.

If we introduce the atomic injection rate r and use the technique described in Sargent et al. (1974) to sum over all atoms, we obtain for the total steady state susceptibility defined by

$$\chi = \chi' + i\,\chi'' = -\frac{\wp^2}{\epsilon_0 \hbar V}\frac{\rho_{ab}}{\Omega}, \tag{4}$$

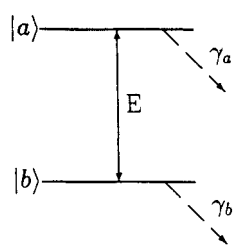

Figure 3: Level scheme for the two-level scheme.

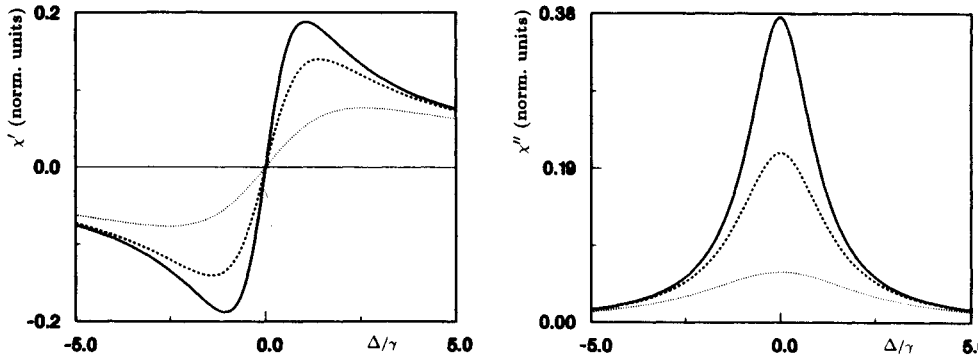

Figure 4: Real (a) and imaginary part (b) of the susceptibility as functions of the detuning in the two-level scheme. Plotted is $\chi\left(\wp^2 r/\left(\epsilon_0\hbar\gamma^2 V\right)\right)^{-1}$. Note that in our formalism the atomic number density is given by $N = r/\gamma V$ with the cavity volume V. The parameters are $\gamma_a = 0.1\gamma$, $\gamma_b = 2\gamma$, $\rho^0_{aa} = 0.01$, and $\rho^0_{bb} = 0.99$. The three curves correspond to field amplitudes of $\Omega = 0.01\gamma$ for the solid curve, $\Omega = 0.2\gamma$ for the dashed curve and $\Omega = 0.5\gamma$ for the dotted curve.

where ρ is now the sum over the density matrices of all atoms in the cavity and $\Omega = \wp E/\hbar$ is the Rabi-frequency of the field,

$$\chi' = \frac{\wp^2 r}{\epsilon_0\hbar V}\left(\frac{\rho^0_{bb}}{\gamma_b} - \frac{\rho^0_{aa}}{\gamma_a}\right)\frac{\Delta_{ab}}{\Delta^2_{ab} + \gamma^2_{ab}\left(1 + \frac{4|\Omega|^2}{\gamma_a\gamma_b}\right)}, \tag{5}$$

$$\chi'' = \frac{\wp^2 r}{\epsilon_0\hbar V}\left(\frac{\rho^0_{bb}}{\gamma_b} - \frac{\rho^0_{aa}}{\gamma_a}\right)\frac{\gamma_{ab}}{\Delta^2_{ab} + \gamma^2_{ab}\left(1 + \frac{4|\Omega|^2}{\gamma_a\gamma_b}\right)}. \tag{6}$$

Here V is the interaction volume and ρ^0_{aa} and ρ^0_{bb} are the initial populations of the levels $|a\rangle$ and $|b\rangle$.

The real and imaginary parts of the susceptibility are plotted in figure 4 for different intensities. To achieve high nonlinearities, we would have to tune the probe-field near to the atomic resonance. Near resonance, however, the absorption is also very high, so that the probe-field would of course be absorbed after a short interaction length. But by employing atomic coherences, we can introduce a point of zero absorption in the spectrum near resonance and at the same time maintain the behaviour of the refractive susceptibility.

3 Phaseonium

We now consider the atomic scheme shown in figure 5. A three-level atom is initially prepared in a coherent superposition of the two lower levels $|b\rangle$ and $|b'\rangle$. This can be achieved for example by a coherent pulse excitation. It has been shown by Scully (1991), that the initially prepared coherence together with a small population in the excited state can lead